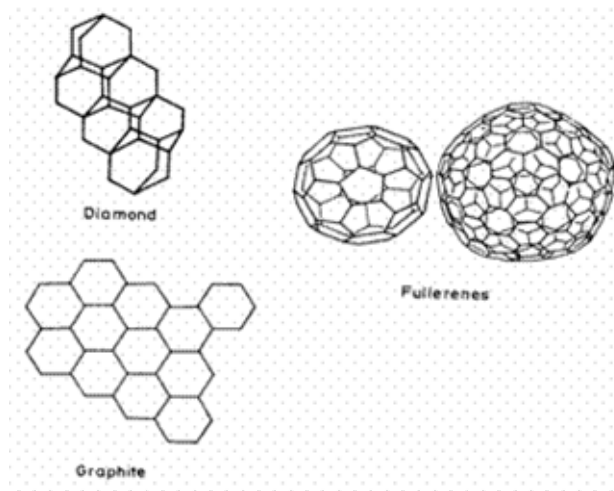
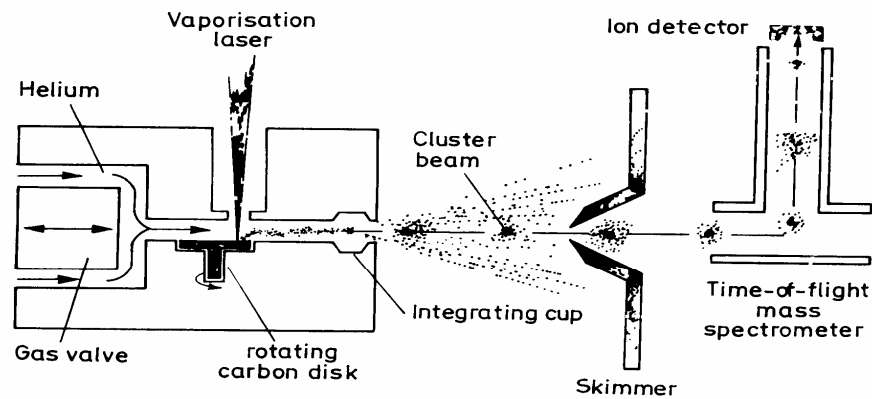


## Chapter - 3

# DIVERSITY IN NANOSYSTEMS



**Figure 1.** A schematic representation of the structures of graphite, diamond and fullerenes. While the two dimensional sheets formed by hexagons are packed one over another in graphite, the diamond structure is three dimensional. Only two fullerenes are shown. The smaller one is buckminsterfullerene, C<sub>60</sub>. The bonds between hexagons are more like double bonds showing the corannulene-type substructure. The double bonds are localised exocyclic to the pentagons giving [5]radialene character to the pentagons and cyclohexa-1,3,5-triene character to the hexagons.



**Figure 2.** The experimental set-up used to discover C<sub>60</sub>. The graphite disk is evaporated with a Nd:YAG laser and the evaporated carbon plasma is cooled by a stream of helium coming from a pulsed valve. The clusters of carbon are produced in the integration cup and are expanded into vacuum. The ions are detected by time of flight mass spectrometry ( For a historical review of this area see, Hugh Aldersey-Williams, *The Most Beautiful Molecule, The Discovery of the Buckyball*, John Wiley and Sons, Inc., New York, 1995).

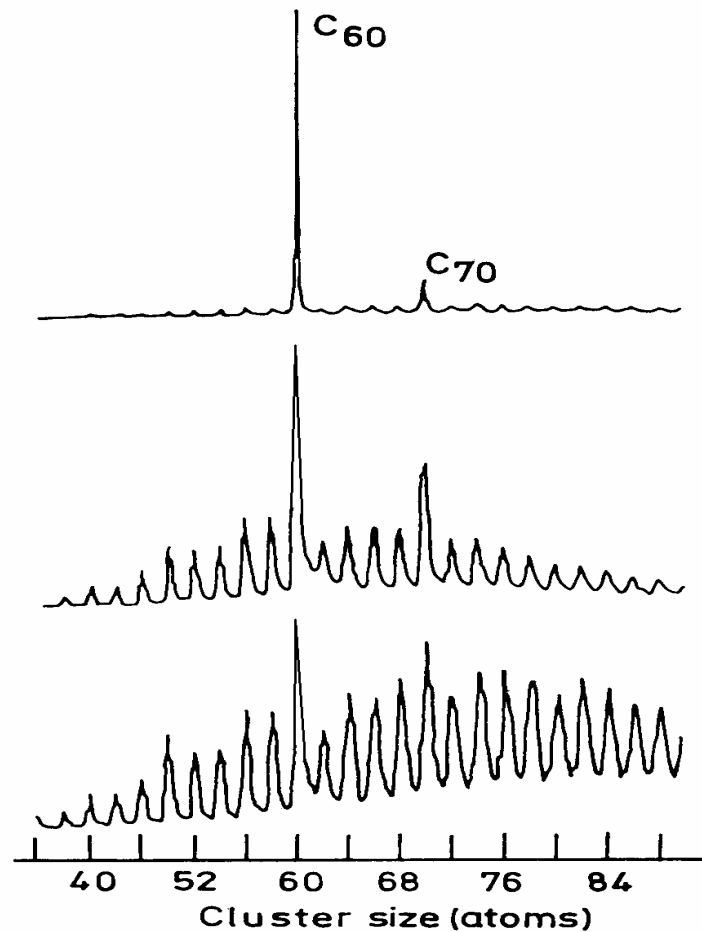


**Figure 3.** The mass spectrum of the carbon clusters under various experimental conditions. Under certain conditions, only C<sub>60</sub> and C<sub>70</sub> are seen ( For a historical review of this area see, Hugh Aldersey-Williams, *The Most Beautiful Molecule, The Discovery of the Buckyball*, John Wiley and Sons, Inc., New York, 1995).

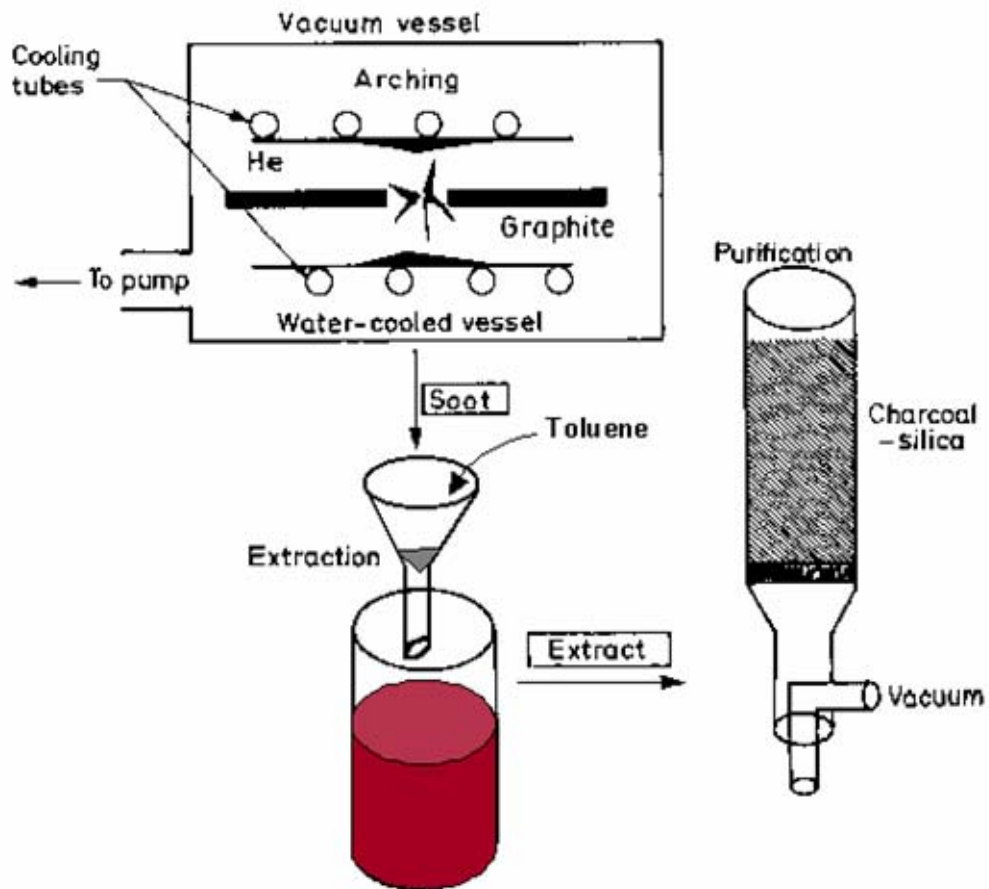
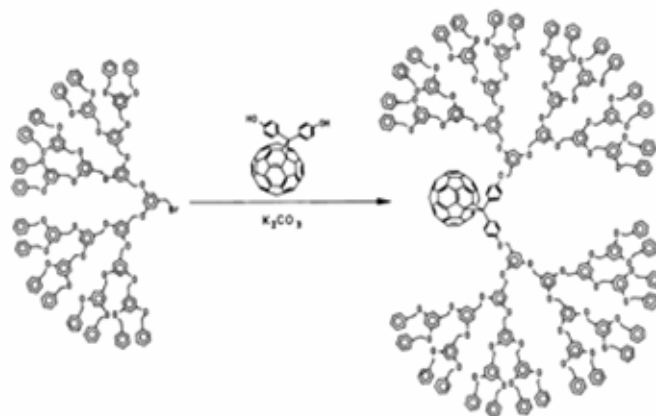
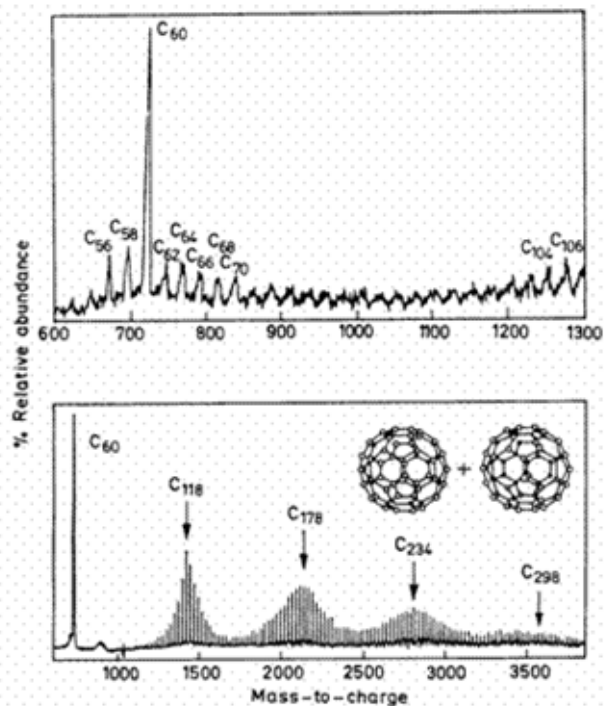


Figure 4. Schematic illustration of the processes involved in the synthesis and purification of fullerenes. Graphite rods are evaporated in an arc, under He atmosphere. The soot collected is extracted with toluene and subjected to chromatography.



**Figure 5.** Schematic showing the synthesis of dendritic methanofullerene, using the established dendritic growth procedures ( K. L. Wooley, C. J. Hawker, J. M. J. Frechet, F. Wudl, G. Sardanov, S. Shi, C. Li and M. Rao, J. Am. Chem. Soc. 115 (1993) 9836).



**Figure 6. (Bottom)** Mass spectrum of a laser evaporated C<sub>60</sub> film showing coalescence of fullerenes. Mass peaks are seen at (C<sub>60</sub>)<sub>n</sub> ( C.Yeretian, K. Hansen, F. Diedrich and R. L. Whetten, Nature 359 (1992) 44). **(Top)** Collision of high energy ions on C<sub>60</sub> results in the addition of C<sub>2</sub>s to C<sub>60</sub>. The mass spectrum here shows the addition of a number of such species ( T. Pradeep and R. G. Cooks, Int. J. Mass Spectrom. Ion Process 135 (1994) 243). Combined figure originally published in, T. Pradeep, Current Science, 72 (1997) 124.

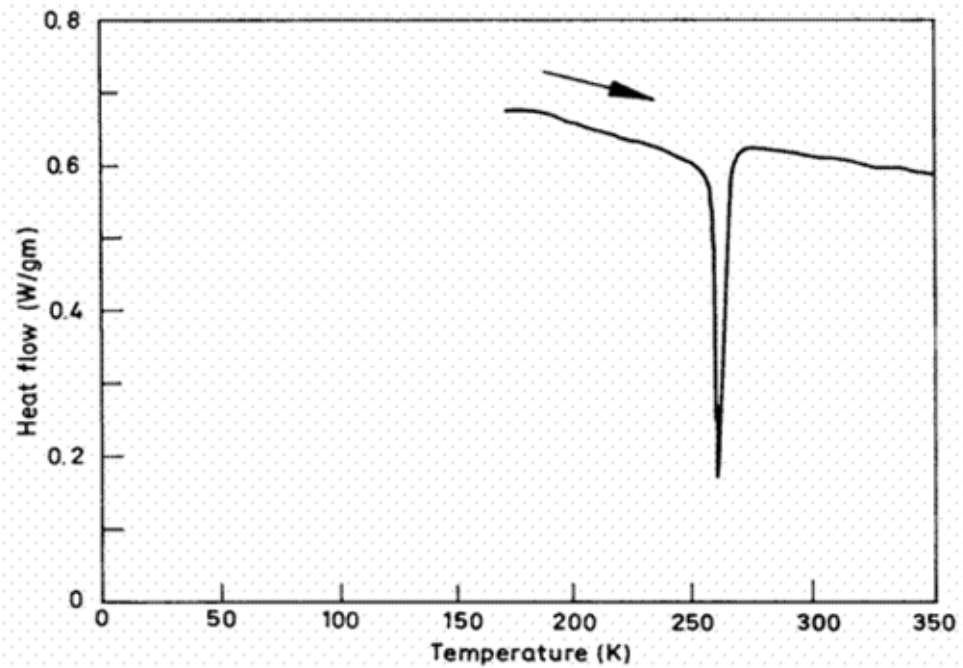


**Figure 7.** Results of a different scanning calorimetric measurement of a powder sample of  $C_{60}$ . The arrow indicates that the data were taken upon warming ( P. A. Heiney, J. E. Fischer, A. R. McGhie, W. J. Romanow, A. M. Denenstein, J. P. McCauley Jr. and A. B. Smith III, *Phys. Rev. Lett.* 66 (1991) 2911 ).



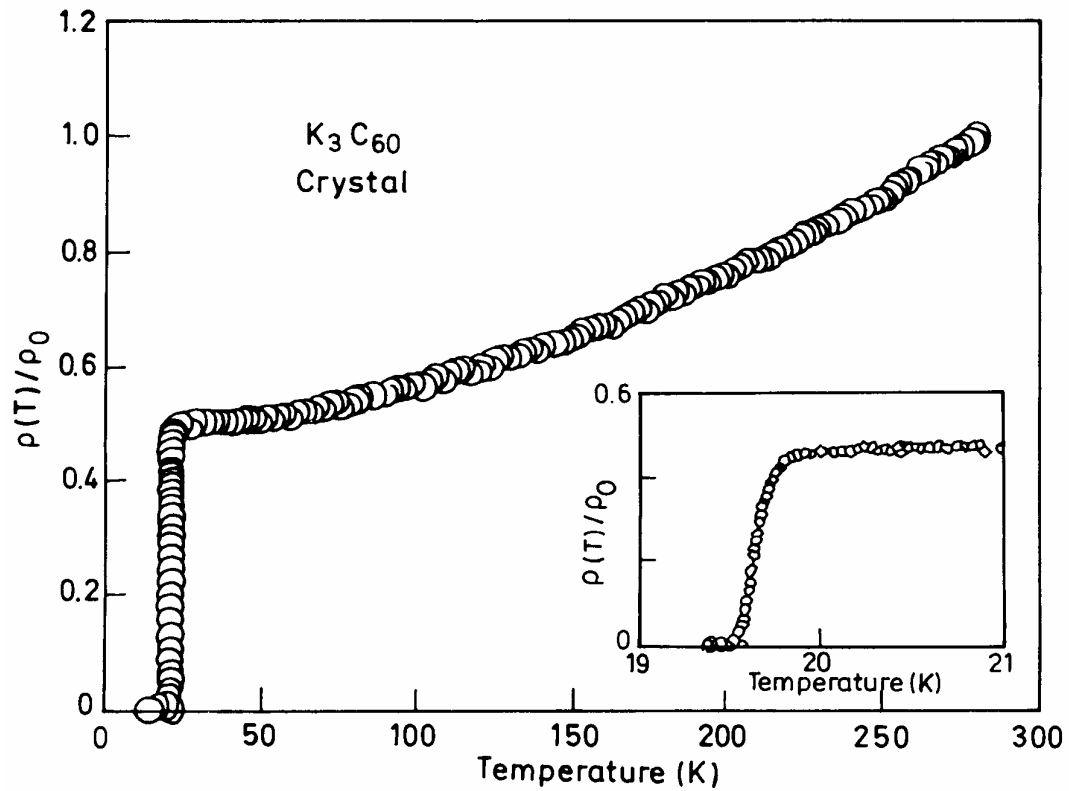


**Figure 8.** Normalised DC electrical resistivity  $\rho(T)$  of a  $K_3C_{60}$  single crystal. The  $T_c$  observed is 19.8K.  $\rho_0$  is the resistivity at  $T=280$  K (X. D. Xiang, J. G. Hou, G. Briceno, W. A. Vareka, R. Mostovoy, A. Zettl, V. H. Crespi and M. L. Cohen, Science 256 (1992) 1190).